



Titre: Temperature and oxygen adsorption coupling effects upon the
Title: surface tension of liquid metals

Auteurs: Aïmen E. Gheribi, & Patrice Chartrand
Authors:

Date: 2019

Type: Article de revue / Article

Référence: Gheribi, A. E., & Chartrand, P. (2019). Temperature and oxygen adsorption
Citation: coupling effects upon the surface tension of liquid metals. Scientific Reports, 9(1),
7113 (9 pages). <https://doi.org/10.1038/s41598-019-43500-3>

 **Document en libre accès dans PolyPublie**
Open Access document in PolyPublie

URL de PolyPublie: <https://publications.polymtl.ca/4888/>
PolyPublie URL:

Version: Version officielle de l'éditeur / Published version
Révisé par les pairs / Refereed

Conditions d'utilisation: CC BY
Terms of Use:

 **Document publié chez l'éditeur officiel**
Document issued by the official publisher

Titre de la revue: Scientific Reports (vol. 9, no. 1)
Journal Title:

Maison d'édition: Nature
Publisher:

URL officiel: <https://doi.org/10.1038/s41598-019-43500-3>
Official URL:

Mention légale:
Legal notice:

SCIENTIFIC REPORTS



OPEN

Temperature and oxygen adsorption coupling effects upon the surface tension of liquid metals

Aïmen E. Gheribi & Patrice Chartrand

An accurate knowledge of the surface tension of liquid metals is critical for many theoretical and practical applications, especially in the current context of emerging growth of nanotechnology. The surface tension and its temperature dependence are drastically influenced by the level of impurities in the metal such as oxygen, sulphur or carbon. For this reason, experimental surface tension data of metals reported in literature are scattered. Strictly speaking, when referring to the surface tension of liquid metals, both variables temperature and oxygen content must be specified. There exists no clear formalism describing the coupling effect temperature and the oxygen content upon the surface tension of liquid metals. The aim of this work is to fill this gap. A thermodynamically self-consistent formulation for the surface tension of liquid metals and semiconductors as a function of temperature and oxygen content is established. According to the proposed formalism, a reliable expression for the surface tension of pure and oxygen saturated metals is then derived. The proposed model is found to be in good agreement with available experimental data, showing a good predictive capability. Aluminium is chosen and thoroughly evaluated as a case study, due to its very high sensitivity to oxygen level. Its surface tension is explicitly formulated as a function of temperature and oxygen content.

Although the surface tension of liquid metals has been extensively studied for nearly a century, both from an experimental and a theoretical point of view, there is still no clear value of the surface of tension liquid metals. In general, the surface tension decreases linearly with temperature:

$$\sigma(T) = \sigma^0(T_m) - \sigma'(T - T_m) \quad (1)$$

where σ^0 and $\sigma' = (\partial\sigma/\partial T)_{T_m}$ denote respectively the surface tension and its temperature derivative, assumed to be constant, at T_m (melting temperature). Equation 1 has proven reliable in a wide range of temperature, a least up to $T_C/2$, T_C being the critical temperature. The experimental values of both σ^0 and σ' reported in the litterature are often scattered, not only because of the errors inherent to experimental methods, but also because they are strongly influenced by the presence of impurities at the surface of the liquid. For instance, the reported value of σ^0 for aluminium is very often: 0.85 N.m^{-1} . However, this value is not for pure aluminum but for aluminium saturated in oxygen. Indeed, because Al and O have a strong chemical affinity, a few ppm of O_2 reacts with Al to form an Al_2O_3 monolayer at the surface. The oxide monolayer causes a drastical decrease of the surface tension, from $1.05 \pm 0.05 \text{ N.m}^{-1}$ to $0.85 \pm 0.05 \text{ N.m}^{-1}$ ^{2,3}. This example reflects the surface tension's extreme sensitivity to oxygen, and more generally to impurities such as S, C, P. This could impact the alloy and process design of many industrial applications, in particular those in a controlled atmosphere. In the literature, several studies report a value of σ' , however no consensus can be established as there is a dispersion of over 100% in reported data¹. Inconsistencies in experimental data cannot be harmonized by a critical assessment as the impurity content must be considered as a variable. The primary purpose of this work is to establish a clear and reliable formalism to describe the surface tension as a function of both temperature and oxygen content.

In our recent work, considering the Gibbs adsorption isotherm concept, we have shown that the oxygen content (x_o) dependence upon surface tension can be by first degree approximation assumed to be directly proportional to the value of the surface tension at a given temperature: $(\partial\sigma/\partial x_o) \propto \sigma$. By integration, the following expression has been formulated⁴:

CRCT - Polytechnique Montréal, Chem. Eng., Box 6079, Station Downtown, Montréal, Qc, H3C 3A7, Canada. Correspondence and requests for materials should be addressed to A.E.G. (email: aimen.gheribi@polymtl.ca)

$$\sigma(T, x_O) = \sigma_{pure}(T) \left[1 - \lambda_O^{sat} \Gamma_O^{sat} \left(1 - e^{-\xi_O \frac{x_O}{x_O^{sat}(T)}} \right) \right] \quad (2)$$

where Γ_O^{sat} and x_O^{sat} are respectively the full coverage oxygen adsorption at the liquid surface and the oxygen content at full coverage (saturation). Both parameters λ_O^{sat} and ξ_O are universal constants, i.e. identical for all elements. Their values were determined by Gheribi *et al.*⁴ as: $\lambda_O^{sat} = 16078$ and $\xi_O = 7.422$. Γ_O^{sat} can be determined from the lattice constants of the corresponding metal-oxyde monoxide using the well established Kozakevitch's approximation given by⁵:

$$\Gamma_O^{sat} = \frac{n_O}{A \cdot N_A} \quad (3)$$

where A is the mesh surface, n_O the number of oxygen at the mesh surface and N_A the Avogadro number. For monoxide, $n_O = 2$. In practice, A is defined as $(n_c \cdot V_m, o \cdot N_A^{-1})^{\frac{2}{3}}$, with $V_{m,o}$ and n_c respectively the molar volume of the monoxide at standard temperature (298.15 K) and the number of atoms per unit cell⁶. In a nutshell, in this formalism (Eq. 2) there is no adjustable parameter, provided that $\sigma^0(T)$ and x_O^{sat} are known. x_O^{sat} is determined from phase equilibria and crystallographic data and in general it is known with an appreciable accuracy while $\sigma^0(T)$ is not well defined for most elements, especially those with a significant reactivity with oxygen. Indeed, most of the time, the reported values for $\sigma^0(T)$ are underestimated, as they are related to experiments performed with contaminated samples (with non-metallic impurities, in particular oxygen). In practice, there is no clear formalism describing the surface tension of pure elements as a function of temperature but also the temperature-impurities content coupling effect upon the surface tension of metals. Naturally, several assessments and recommended parameters for Eq. 1 can be found in the litterature, see e.g.^{1,7-10}, however none of them clearly recommends values for temperature dependent surface tension for pure metals.

Thermodynamically consistent formulation of the temperature dependence of the surface tension

Let us consider a pure element, from a thermodynamic point of view. The temperature derivative of the surface tension defines the excess surface entropy, ΔS^{s11} :

$$\left(\frac{\partial \Delta S^s}{\partial A} \right)_{T,P} = - \left(\frac{\partial \sigma}{\partial T} \right)_{A,P} = - \left(\frac{\partial}{\partial T} \left(\frac{\partial \Delta F^s}{\partial A} \right)_{T,A} \right) \quad (4)$$

where A and ΔF^s are respectively the surface and the excess surface Helmholtz free energy. The molar surface, A_m , is expressed as¹² $A_m = L \cdot N_A^{1/3} \cdot V_m^{2/3}$, where L is a factor taking into account the packing of the liquid, N_A is the Avogadro number and V_m the molar volume. L lies in general between 1.04 and 1.12, however the generic value of 1.09 is generally used, corresponding to the packing factor of close-packed structures. Then:

$$\left(\frac{\partial \sigma}{\partial T} \right)_{A,P} = - \frac{1}{LN_A^{1/3}} \left(\frac{\partial}{\partial T} \left(\frac{\partial \Delta F_m^s}{\partial V_m^{2/3}} \right)_{T,A} \right) \quad (5)$$

Without loss of generality it can be assumed that the surface and the bulk Helmholtz free energy are proportional, i.e. $F_m^s \propto \Delta F_m$. Neglecting the difference between the bulk and the surface electronic structure, this proportionality can be expressed as¹³:

$$\Delta F_m^s = \left(\frac{Z_S - Z_B}{Z_B} \right) F_m \quad (6)$$

where Z_B and Z_S are respectively the bulk and the surface coordination. Then we denote the ratio $(Z_B - Z_S)/Z_B$ by β . Thereafter, given that the Maxwell relations define $(\partial^2 F_m / \partial V \partial T)$ as the product: $\alpha_V B_T$ ¹⁴ where α_V and B_T are the volumetric thermal expansion and the isothermal bulk modulus, Eq. 5 can be rewritten as:

$$\left(\frac{\partial \sigma}{\partial T} \right)_{A,P} = - \frac{3\beta}{2LN_A^{1/3}} V_m^{1/3} \alpha_V B_T \quad (7)$$

Note that the product $\alpha_V \cdot B_T$ is defined as the thermal pressure coefficient. For liquid and solid metallic or semiconductors elements, the thermal pressure coefficient is nearly independent of temperature¹⁵, thus $(\partial \sigma / \partial T)_{A,P}$ is a constant that can be written as σ'_{pure} . In general, for liquid metals, the generic average of $L = 1.091$ is used¹⁶, then one can define:

$$\sigma'_{pure}(T) = -1.628 \times 10^{-8} \beta V_m^{1/3} \alpha_V B_T \quad (8)$$

where β characterises the ratio of “broken bonds” at the surface compared to the bulk and should be specific for each element as, contrary to crystals, the bulk coordination of liquid metals varies between elements. For FCC and BCC crystals, it is well known that $\beta = 0.25$. For bulk liquid metals the average coordination number is

10.35 ± 0.06 ^{17,18}. If, as suggested by Kaptay *et al.*¹⁹, we assume that surface liquid metals are structured similarly to the (1 1 1) FCC lattice plane with $Z_s = 9$, the average value of β should be as follows:

$$\langle \beta \rangle \simeq 0.132 \pm 0.045 \quad (9)$$

This value is close to $\beta = 1/6$ and $\beta = 0.174 \pm 0.023$ proposed respectively by Oriani²⁰ and Kaptay *et al.*¹⁹.

As mentioned before, the surface tension of pure metals at melting temperature, σ_{pure}^0 , is not precisely known. In fact, little data is available. One of the advantages of the Gheribi *et al.* formalism⁴ is that the surface tension of pure liquid metals and its temperature dependence can be deduced directly from those of oxygen saturated ones. Indeed, according to Eq. 2:

$$\frac{\sigma_{pure}(T_m)}{\sigma_{sat}(T_m)} = \frac{\sigma'_{pure}(T_m)}{\sigma'_{sat}(T_m)} = \frac{1}{1 - \lambda_O^{sat} \Gamma_O^{sat}} \quad (10)$$

where σ_{sat} and σ'_{sat} are the surface tension of the oxygen saturated liquid metal and its temperature derivative assumed constant. In our recent publication⁴, we demonstrated the reliability of Eq. 9 by predicting the surface tension drop between pure and oxygen saturated metals for several case studies. The fact that in the present formalism the product $\lambda_O^{sat} \Gamma_O^{sat}$ governs the variation of both σ and σ' at oxygen saturation is not surprising. Indeed, the model describing the oxygen content effect upon the surface tension (Eq. 2) originates from the assumption that $(\partial\sigma/\partial x_O) \propto \sigma$. From a thermodynamic point of view, the excess surface entropy has two contributions: (i) a vibrational contribution due to the difference of quasi-lattice vibration at the bulk and surface, ΔS_{vib}^s , and (ii) a configurational contribution, ΔS_{conf}^s , due to the presence of impurities at the surface. Then, one can define:

$$\left(\frac{\partial\sigma}{\partial T} \right)_{A,P} = - \frac{(\Delta S_{vib}^s + \Delta S_{conf}^s)}{A_m} \quad (11)$$

Thereby, the two contributions of excess surface entropy can be defined by identifying Eq. 11 to Eq. 7 and Eq. 10:

$$\begin{aligned} \Delta S_{vib}^s &= \frac{3}{2} \beta V_m \alpha_V B_T \\ \Delta S_{conf}^s &= -\lambda_O^{sat} \Gamma_O^{sat} \Delta S_{vib}^s \end{aligned} \quad (12)$$

The excess vibrational surface entropy is positive while the excess configurational surface entropy is negative. This is in agreement with the principles of statistical physics¹². In the present formalism, both the vibrational and configurational excess entropies are correlated. This is also consistent with the Skapski^{12,13} formalism of the surface entropy. Indeed, from statistical mechanics principles, Skapski derived an expression for the excess configurational and vibrational surface entropy, demonstrating that both contributions can be approximated by functions depending only on the ratio between the average bulk and surface coordination numbers. This can be explained by the fact that the main contribution for the difference between the thermodynamic properties of bulk and surface is the difference between the coordination. Eq. 12 is, to some extent, consistent with the Skapski formalism as the vibrational and configurational excess entropies are intercorrelated via β .

In a nutshell, according to the present formalism, one can **predict**:

- the temperature dependence of the surface tension of pure and oxygen saturated liquid metals
- the surface tension of pure liquid metals at melting point from its oxygen saturated surface tension
- the surface tension of liquid metals as a function of temperature and oxygen content from the knowledge of the surface tension of oxygen saturated metals at the melting point

It should be noted that the measure of the solubility of oxygen in liquid metals can be either obtain from e.m.f. measurements²¹ or by electrochemical methods such as described in^{22,23}.

Results and Discussion

Let us now validate the formalism. For 20 liquid metals, we compare the experimental temperature dependence of the surface tension of pure or “nearly” pure elements with predictions by Eq. 8. The purest experimental data were chosen as samples for experiments. In addition, chosen experimental data must have been reported in a quite large range of temperatures, ≥ 200 K. To calculate the thermal pressure coefficient, we have considered the critically assessed density, thermal expansion, heat capacity (C_p) and velocity of sound (C_0) (references are given in Table 1). The density of liquid metals varies linearly with temperature: $\rho(T) = \rho^0 - \rho'(T - T_m)$. Then, at the melting temperature, thermal expansion is: ρ'/ρ^0 and the isothermal bulk modulus is deduced from the velocity of sound according to the relation: $B_T = (c_0^2 \rho)/(1 + \alpha_V \gamma T)$, where γ is the Grüneisen parameter defined as $\gamma = (\alpha_V V_m^2 C_p)/(C_0^2 M)$, M being the molecular weight.

Table 1 presents the predicted and the experimental temperature dependence coefficients of the surface tension for 20 pure liquid metals, along with the corresponding surface tension at melting temperature. The physical properties needed to calculate the thermal pressure coefficient ($\alpha_V B_T$) and thus to predict σ'_{pure} are also reported. Figure 1 compares the predicted and experimental σ'_{pure} for 20 liquid metals for which reliable experimental data were available. Conservative error bars were assumed to be 25% and 15% respectively for experimental and predicted σ'_{pure} . Error bars for predicted σ'_{pure} come from the uncertainty in ρ' but especially in C_0 as the uncertainty

#	T_m	ρ^0	ρ'	C_0	C_p	$10^4 \times \alpha_v/K$	B_T	$\sigma(Exp.)$	$10^4 \sigma'(Exp.)$	$10^4 \sigma'(Pred.)$
		kg/m ³	kg/(m ³ ·K)							
Si	1683	2550	0.26 ^a	3920 ^f	29.20 ^g	1.04	30.95	0.83 ^h	-1.00	-1.53
Ni	1727	7861	0.99 ^b	4047 ^f	43.08 ^g	1.26	80.02	1.85 ⁱ	-3.64	-4.22
Fe	1811	7035	0.93 ^c	4200 ^f	46.00 ^g	1.32	74.35	1.93 ^j	-4.00	-4.19
Sn	505	6979	0.65 ^d	2464 ^f	29.69 ^g	0.93	38.30	0.61 ^k	-1.70	-1.98
Cu	1356	7997	0.82 ^d	3440 ^f	32.84 ^g	1.02	71.41	1.40 ^l	-3.30	-3.14
Bi	544	10028	1.21 ^b	1640 ^f	30.49 ^g	1.21	23.52	0.38 ^m	-0.70	-1.68
Ag	1234	9264	0.88 ^b	2790 ^f	33.47 ^g	0.95	56.48	0.96 ⁿ	-1.85	-2.60
Co	1766	7827	0.94 ^a	4031 ^f	40.46 ^g	1.20	79.43	1.89 ^o	-3.30	-4.00
Al	934	2377	0.31 ^c	4561 ^f	31.75 ^g	1.31	38.57	1.02 ^p	-2.74	-2.44
Cd	593	8008	1.25 ^a	2256 ^f	29.71 ^g	1.56	31.86	0.66 ^q	-2.50	-2.58
Ga	303	6077	0.61 ^a	2873 ^f	28.47 ^g	1.01	47.24	0.72 ^r	-0.68	-2.30
Ge	1211	5600	0.55	2693 ^f	27.61 ^g	0.98	33.01	0.66 ^s	-1.56	-1.64
In	430	7022	0.76 ^a	2337 ^f	29.48 ^g	1.09	34.58	0.57 ^t	-0.90	-2.05
K	337	838	0.23	1876 ^f	32.16 ^g	2.77	2.66	0.12 ^u	-0.62	-0.57
La	1203	5940	0.61 ^c	2030 ^f	34.31 ^g	1.03	20.23	0.75 ^v	-1.00	-1.28
Na	371	927	0.23 ^c	2526 ^f	31.87 ^g	2.48	5.35	0.21 ^w	-0.50	-0.83
Pb	661	10656	1.24 ^b	1821 ^f	30.45 ^g	1.16	29.90	0.48 ^x	-2.40	-2.01
Ti	1958	4140	0.15 ^c	4309 ^f	47.24 ^g	0.36	64.31	1.56 ^y	-0.62	-1.12
Au	1336	17310	1.34 ^c	2568 ^f	30.96 ^g	0.77	85.37	1.19 ^z	-2.51	-3.20
Sb	904	6467	0.61 ^b	1900 ^f	31.38 ^g	0.94	20.99	0.38 ^z	-0.84	-1.13

Table 1. Critically assessed density (ρ), density temperature dependence coefficient ρ' , average velocity of sound (C_0), heat capacity at constant pressure, (C_p). Both thermal expansion (α_v) and isothermal bulk modulus (B_T) are deduced from ρ , ρ' , C_0 and C_p (see text). The predicted (*Pred.*) temperature dependence coefficient of pure liquid metals (σ') is given in comparison with the experimental ones (*Exp.*) and surface tension at melting point (σ) for supposedly pure metals. References are as follows: ^{a56}, ^{b57}, ^{c58}, ^{d59}, ^{e60}, ^{f24}, ^{g25}, ^{h61}, ⁱ⁶², ^{j63}, ^{k2}, ^{l64}, ^{m65}, ⁿ⁶⁶, ^{o67}, ^{p49}, ^{q68}, ^{r69}, ^{s70}, ^{t45}, ^{u71}, ^{v72}, ^{w73}, ^{x74}, ^{y75}, ^{z76}. Note that references for σ and σ' are identical as they are from the same set of experimental data.

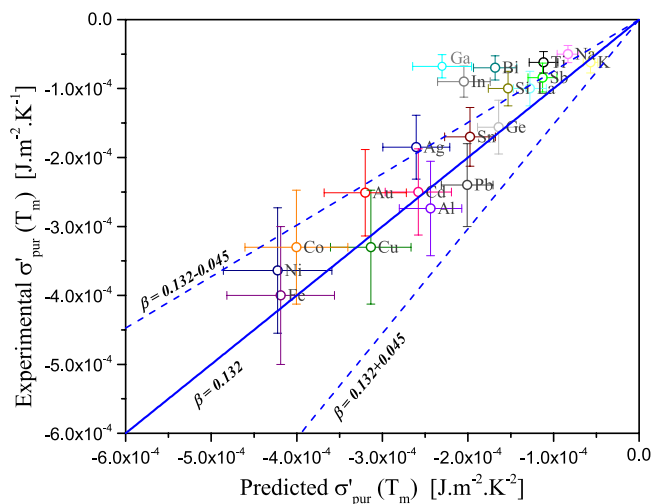


Figure 1. Parity plot representing predicted versus experimental temperature dependence coefficients of the surface tension (σ'_{pure}) for 20 pure liquid metals. The solid line represents the predicted σ'_{pure} via Eq. 8 with the average value of $\beta = 0.132$ while the two dash lines represent the predicted σ'_{pure} with the upper and lower limits of β as defined by Eq. 9. The error bars are determined to be $\pm 25\%$ for experimental σ'_{pure} and $\pm 15\%$ for predicted values.

in C_0 measurements is important²⁴ (10–15%). In general, the agreement between experimental and predicted σ'_{pure} is satisfactory, most of the data are within the model limits represented by the upper and lower values of β . This indicates the reliability of the proposed formalism, i.e. a linear relationship between the temperature dependence coefficient of the surface tension and the thermal pressure coefficient (Eq. 8). The deviation from between the predictions made with $\beta = 0.132$ and experimental data could be explained by a fluctuation of surface

coordination numbers. Indeed, in all likelihood, β should be specific to each element as Z_S and Z_B varies from an element to another. The model accuracy could be improved if surface coordination numbers data were available. For now, the average value of $\beta = 0.132$ is at first glance satisfactory for all liquid metals. It is interesting to note that for Bi, Ga and In the value of β seems to be smaller than that of liquid metals indicating that for these elements, β is smaller, close to 0.066. In other words, for these three elements, the difference between Z_S and Z_B is less pronounced than other liquids metals, a difference of about 6.6%. A better estimation of β for each element is an important issue to explore in the near future as it could improve the model accuracy. That would however require an accurate prediction of surface coordination numbers for each element, via atomistic simulations.

In summary, according to the proposed formalism, **only** the surface tension value at oxygen saturation and the maximum oxygen solubility as a function of temperature are required to predict the surface tension as a function of both temperature and oxygen content. The calculation procedure can be written as follows:

1. Calculate Γ_O^{sat} via Eq. 3 and select from literature (or from thermodynamic database) critically assessed values of x_O^{sat} as a function of temperature
2. Select from literature critically assessed σ_O^{sat} at melting or reference temperature
3. Predict σ_{pure} via Eq. 10
4. Predict σ'_{pure} via Eq. 8
5. Deduce σ^{sat} .
6. Parametrize Eq. 2 and represent $\sigma(T, x_O)$.

As a case study for this procedure, we propose to examine the surface tension of aluminium. Aluminium is the second most produced metal in the world. Controlling the surface tension of aluminium and aluminium alloys is of primary importance in many industrial application. Even though it is well known that oxygen decreases drastically the surface tension of aluminium, there exists in the literature no clear formulation of the surface tension of aluminium as a function of both temperature and oxygen content. Very little of oxygen, (~ 5 ppm in general), is enough to saturate the surface of the liquid with an oxide monolayer. As a result, most experimental data reported in the literature are those of oxygen saturated aluminium. In practice, it is very likely that the oxygen content in the atmosphere is enough to saturate the aluminium surface. However, in some practical and industrial applications, aluminium is free or almost free of oxygen. For instance, in the Hall-Héroult aluminium electrolyse cells, the liquid metal pad is free or nearly of oxygen.

Following the procedure given above, let us formulate and examine the surface tension of aluminium versus T and x_O . From the aluminium monoxide lattice parameters, we estimated, in our prior work, that $\Gamma_0^{sat} = 1.65 \times 10^{-5}$ mol.m⁻². x_O^{sat} as a function of temperature is available in the FactSage thermodynamic software and databases²⁵ and it can be represented by the following expression:

$$x_O^{sat}(T)[ppm] = 5.0 \times 10^{-5} + e^{11.265 - \frac{10964}{T}} \quad (13)$$

According to the most recent assessments^{10,26,27}, the surface tension of oxygen saturated liquid aluminium at the melting temperature (933 K) is: σ_O^{sat} . 0.86 J.m⁻². Then $\sigma(T, x_O)$ is predicted.

First, let us examine the calculated surface tension as a function of both temperature and oxygen content, represented in Fig. 2 at up to 1500 K. The surface tension follows an irregular shape, showing a pronounced asymmetry. At low temperature, close to the melting temperature, the surface tension shows an abrupt decrease with oxygen content and then becomes constant (σ_O^{sat}) whereas at higher temperature, this decrease is smoother and the surface tension reaches σ_O^{sat} at higher oxygen level. The linear behaviour of surface tension with temperature is, strictly speaking, true for pure and oxygen saturated liquid metals. The predicted surface tension of pure and oxygen saturated liquid aluminium is given by the following expressions:

$$\begin{cases} \sigma_{pure}(T) = 1.16 - 2.44 \times 10^{-4} (T - 933) \quad [J.m^{-2}] \\ \sigma_{sat}(T) = \underbrace{0.86}_{Exp.} - 1.80 \times 10^{-4} (T - 933) \quad [J.m^{-2}] \end{cases} \quad (14)$$

These two equations are parameterized only based on the experimental value of the the surface tension of oxygen saturated metal. In Fig. 3, the surface tension of liquid aluminium at melting temperature (933 K) is represented as a function of oxygen content in comparison with available experimental data. The predicted surface tension of pure Al is in very good agreement with experiments. Our predicted surface tension of 1.16 J.m⁻² is very close to the experimental value reported by Chacon *et al.*²⁸ and Garci-Cardovilla *et al.*³ for pure aluminium. It is important to note that in the case of liquid aluminium, the oxygen saturation is less but close to 5 ppm.

Let us now discuss the core of this work, the coupling effect between the temperature and the oxygen adsorption at the surface of liquid metals. In Fig. 4 we represent the calculated surface tension of pure liquid aluminium (free of oxygen), oxygen saturated and with various levels of oxygen, from 0.1 ppm to 50 ppm. One can see that the proposed model can predict accurately the temperature dependence of saturated oxygen liquid aluminium. It is interesting to note the data dispersion at melting temperature (933 K). Chacon *et al.*²⁸, Pamies *et al.*²⁹, Garcia-Cordovilla³, Saravanan *et al.*³⁰, Anson *et al.*³¹ and to a lesser extent Roach *et al.*³² attempted to measure the surface tension of aluminium more or less successfully. Figure 4 helps to understand the discrepancy observed in measurements in terms of oxygen content. For instance, data reported by Garcia-Cordovilla³ and Pamies *et al.*²⁹ correspond to the surface tension of liquid aluminium containing 0.1 ppm oxygen while those reported by Roach *et al.*³² contain about 1 ppm. When considering the reported oxygen level, experimental datasets for supposedly

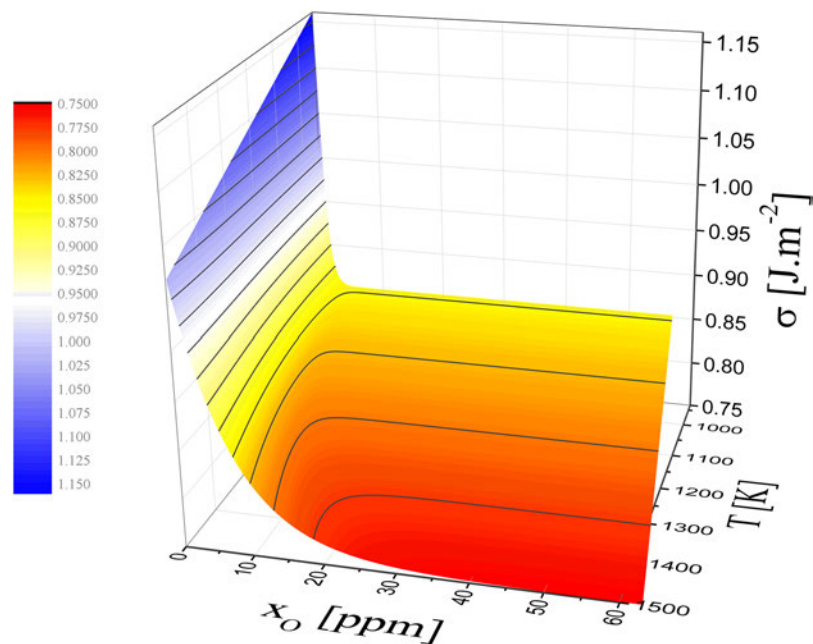


Figure 2. Predicted, via Eq. 8, surface tension of liquid aluminium as a function of temperature and oxygen content. Parameters for Eq. 8: $\Gamma_0^{sat} = 1.65 \times 10^{-5} \text{ mol.m}^{-2}$, $\sigma_0^{sat} = 0.86 \text{ J.m}^{-2}$ and x_0^{sat} is a function of temperature calculated by Eq. 13.

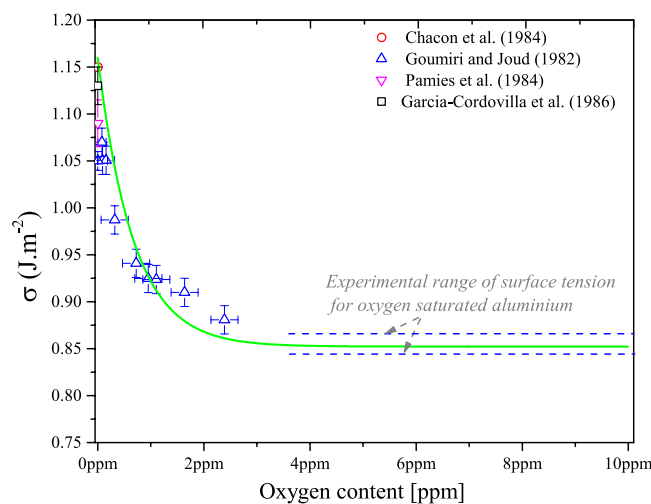


Figure 3. Predicted surface tension of liquid aluminium as a function of oxygen content at melting temperature (933 K) (solid line) in comparison with experimental data at the same temperature (open symbols). References: Chacon *et al.*²⁸, Goumiri and Joud², Pamies *et al.*²⁹, Garcia-Cordovilla *et al.*³. The two dash lines represent the standard deviation of the mean experimental surface tension of oxygen saturated aluminium^{1,10,26,27}.

pure liquid aluminium become consistent with each other. The shape of the oxygen content dependence upon the surface tension is particular: it is similar to a cumulative distribution function. In others words, $(\partial\sigma/\partial x_O)$ is described by a peak function of temperature. The peak is positioned where the composition of x_O becomes smaller than x_0^{sat} . When the liquid metal is saturated in oxygen, the surface tension obeys $\sigma(T) = \sigma_0^{sat}(T_m) - \sigma'_{sat}(T)$, but as the temperature rises the oxygen content could, at a certain temperature, be less than the maximum oxygen solubility in the liquid metal. As a result, above this temperature, the liquid metal could start adsorbing oxygen again, leading to an increase of its surface tension.

The good predictive capability of the proposed model when predicting the surface tension of liquid aluminium as a function of both temperature and oxygen content was clear. Naturally, the same theoretical treatment can be employed to predict the surface tension of other transition metals, as functions of T and x_O . The predictive capability of the model is expected to be good for other metals, as the reliability of Eq. 1 has been already proven for a large number of elements in our prior work⁴.

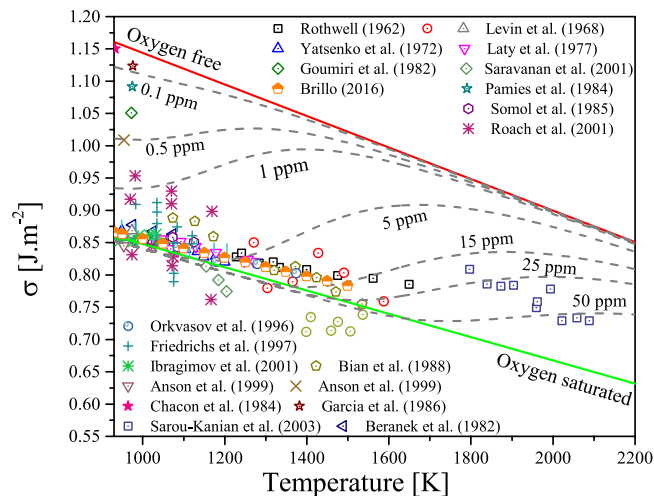


Figure 4. Predicted surface tension of liquid aluminium as a function of temperature for pure (upper solid line), oxygen saturated (lower solid line) and various iso-oxygen contents (dashed lines) from 0.1 to 50 ppm in comparison with available experimental data (open symbols). Note that data reported by Chacon *et al.*³, Pamies¹⁹⁸⁴, Garcia-Cordovilla *et al.*³, Anson *et al.*³¹ are assumed to be for pure or nearly pure liquid aluminium. Experimental data are referenced as follow: Levin *et al.*⁴⁴, Yatsenko *et al.*⁴⁵, Brillo *et al.*⁴⁶, Laty *et al.*⁴⁷, Pamies *et al.*²⁹, Somol *et al.*⁴⁸, Sarou-Kanian *et al.*⁴⁹, Rothwell⁵⁰, Goumiri *et al.*², Saravanan *et al.*³⁰, Roach *et al.*³², Orkvasov *et al.*⁵¹, Friedrichs *et al.*⁵², Ibragimov *et al.*⁵³, Anson *et al.*³¹, Bian *et al.*⁵⁴, Garcia-Cordovilla *et al.*³, Beranek *et al.*⁵⁵, Chacon *et al.*²⁸.

Conclusion

In conclusion, we presented in this work a thermodynamically self consistent approach to predict the coupling effects between the temperature and adsorbed oxygen upon the surface tension. The model has proven to have a good predictive capability by predicting the temperature dependence of surface tension for several liquid metals (Table 1 and Fig. 1). The proposed method could be useful for current research, for example in Integrated computational materials engineering (ICME) for alloys and process design^{33–35}. Indeed, the proposed formalism shows that the surface tension versus T and x_O is intercorrelated with other physical properties: thermal expansion, velocity of sound, heat capacity and oxygen solubility. When building a property database, one can now also consider the surface tension to ensure self consistency between the physical properties. Having more reliable databases lead to better predictions of properties for which few or no experimental data are available. A similar approach was successfully employed to couple thermal thermodynamics and thermal transport properties^{36–40}. Lastly, for some liquid metals, due to their significant reactivity with non metallic impurities (O_2 , S, P, C, etc.), it is difficult to measure the surface tension of the pure elements. In a near future, utilising molecular dynamic simulation campaigns based on reliable Modified Embedded Atom Model (MEAM)^{41–43}, the surface tension of several liquid metals will be predicted in order to confirm the validity of Eq. 10.

Data Availability

All data generated or analysed during this study are included in this published article.

References

- Keene, B. J. Review of data for the surface tension of pure metals. *Int. Mater. Rev.* **38**, 157–92, <https://doi.org/10.1179/imr.1993.38.4.157> (1993).
- Goumiri, L. & Joud, J. C. Auger electron spectroscopy study of aluminum-tin liquid system. *Acta Metall.* **30**, 1397–405, [https://doi.org/10.1016/0001-6160\(82\)90160-2](https://doi.org/10.1016/0001-6160(82)90160-2) (1982).
- Garcia-Cordovilla, C., Louis, E. & Pamies, A. The surface tension of liquid pure aluminium and aluminium-magnesium alloy. *Journal of Materials Science* **21**, 2787–2792, <https://doi.org/10.1007/BF00551490> (1986).
- Gheribi, A. E., des Roches, M. V. & Chartrand, P. Modelling the surface tension of liquid metals as a function of oxygen content. *Journal of Non-Crystalline Solids* **505**, 154–161, <http://www.sciencedirect.com/science/article/pii/S0022309318305842>, <https://doi.org/10.1016/j.jnoncrysol.2018.10.006> (2019).
- Kozakevitch, P. Surface activity in liquid metal solutions. *SCI (Soc. Chem. Ind., London) Monogr. No.* **28**, 223–45 (1968).
- Ozawa, S., Nishimura, M. & Kuribayashi, K. Surface tension of molten silver in consideration of oxygen adsorption measured by electromagnetic levitation. *International Journal of Microgravity Science and Application* **33**, 3303010–3303016, <http://www.jasma.info/journal/?report=surface-tension-of-molten-silver-in-consideration-of-oxygen-adsorption-measured-by-electromagnetic-levitation>, <https://doi.org/10.15011/jasma.33.330310> (2016).
- Haynes, W. *CRC Handbook of Chemistry and Physics*. (CRC Press, 2016).
- Egry, I., Ricci, E., Novakovic, R. & Ozawa, S. Surface tension of liquid metals and alloys—recent developments. *Advances in Colloid and Interface Science* **159**, 198–212, <http://www.sciencedirect.com/science/article/pii/S0001868610001223>, <https://doi.org/10.1016/j.cis.2010.06.009> (2010).
- Iida, T. & Guthrie, R. I. The physical properties of liquid metals. Clarendon Press, Walton Street, Oxford OX 2 6 DP, UK, 1988 (1988).
- Brillo, J. *Thermophysical properties of multicomponent liquid alloys*. (Walter de Gruyter GmbH & Co KG, 2016).
- Guggenheim, E. A. *Thermodynamics: an Advanced Treatment for Chemists and Physicists. 6th Ed.* (North-Holland Publishing Co., 1977).
- Skapski, A. S. The temperature coefficient of the surface tension of liquid metals. *The Journal of Chemical Physics* **16**, 386–389, <https://doi.org/10.1063/1.1746896> (1948).

13. Skapski, A. S. The surface tension of liquid metals. *The Journal of Chemical Physics* **16**, 389–393, <https://doi.org/10.1063/1.1746898> (1948).
14. Gheribi, A. E. Formulation of the thermal volume consistent with swenson's concept of thermal pressure. *Physics of the Earth and Planetary Interiors* **177**, 59–64, <http://www.sciencedirect.com/science/article/pii/S0031920109001538>, <https://doi.org/10.1016/j.pepi.2009.07.009> (2009).
15. Harder, J. M., Silbert, M., Yokoyama, I. & Young, W. H. The thermal pressure coefficients and heat capacities of simple liquid metals. *Journal of Physics F: Metal Physics* **9**, 1005 <http://stacks.iop.org/0305-4608/9/i=6/a=007> (1979).
16. Tanaka, T. & Iida, T. Application of a thermodynamic database to the calculation of surface tension for iron-base liquid alloys. *Steel Research* **65**, 21–28, <https://doi.org/10.1002/srin.199400921>.
17. Waseda, Y. The structure of liquid transition metals and their alloys. *Inst. Phys. Conf. Ser.* **30**, 230–40 (1976).
18. Tao, D. P. Prediction of the coordination numbers of liquid metals. *Metallurgical and materials transactions A* **36**, 3495–3497, <https://doi.org/10.1007/s11661-005-0023-5> (2005).
19. Kaptay, G. A unified model for the cohesive enthalpy, critical temperature, surface tension and volume thermal expansion coefficient of liquid metals of bcc, fcc and hcp crystals. *Materials Science and Engineering: A* **495**, 19–26, <http://www.sciencedirect.com/science/article/pii/S0921509308001287>, Fifth International Conference on High Temperature Capillarity HTC-2007, Alicante, Spain (2008).
20. Oriani, R. A. The surface tension of liquid metals and the excess binding energy of surface atoms. *The Journal of Chemical Physics* **18**, 575–578, <https://doi.org/10.1063/1.1747704> (1950).
21. Alcock, C. B. & Belford, T. N. Thermodynamics and solubility of oxygen in liquid metals from e.m.f. measurements involving solid electrolytes. part 1.—lead. *Trans. Faraday Soc.* **60**, 822–835, <https://doi.org/10.1039/TF9646000822> (1964).
22. Roy, P. & Bugbee, B. E. Electrochemical oxygen sensor for measurement of oxygen in liquid sodium. *Nuclear Technology* **39**, 216–218, <https://doi.org/10.13182/NT78-A32081> (1978).
23. Diffusivity, activity and solubility of oxygen in liquid lead and lead–bismuth eutectic alloy by electrochemical methods. *Journal of Nuclear Materials* **349**, 133–149, <http://www.sciencedirect.com/science/article/pii/S0022311505005003>, <https://doi.org/10.1016/j.jnucmat.2005.10.006> (2006).
24. Blairs, S. Sound velocity of liquid metals and metalloids at the melting temperature. *Phys. Chem. Liq.* **45**, 399–407, <https://doi.org/10.1080/00319100701272084> (2007).
25. Bale, C. *et al.* Factsage thermochemical software and databases, 2010–2016. *Calphad* **54**, 35–53, <http://www.sciencedirect.com/science/article/pii/S0364591616300694>, <https://doi.org/10.1016/j.calphad.2016.05.002> (2016).
26. Mills, K. C. & Su, Y. C. Review of surface tension data for metallic elements and alloys: Part 1 pure metals. *International Materials Reviews* **51**, 329–351, <https://doi.org/10.1179/174328006X102510> (2006).
27. Mills, K. C. *Recommended values of thermophysical properties for selected commercial alloys.* (Woodhead Publishing, 2002).
28. Chacon, E., Flores, F. & Navascues, G. A theory for liquid metal surface tension. *Journal of Physics F: Metal Physics* **14**, 1587, <http://stacks.iop.org/0305-4608/14/i=7/a=009> (1984).
29. Pamies, A., Garcia Cordovilla, C. & Louis, E. The measurement of surface tension of liquid aluminum by means of the maximum bubble pressure method: the effect of surface oxidation. *Scr. Metall.* **18**, 869–72, [https://doi.org/10.1016/0036-9748\(84\)90251-5](https://doi.org/10.1016/0036-9748(84)90251-5) (1984).
30. Saravanan, R. A., Molina, J. M., Narciso, J., Garcia-Cordovilla, C. & Louis, E. Effects of nitrogen on the surface tension of pure aluminium at high temperatures. *Scr. Mater.* **44**, 965–970, [https://doi.org/10.1016/S1359-6462\(00\)00688-6](https://doi.org/10.1016/S1359-6462(00)00688-6) (2001).
31. Anson, J. P., Drew, R. A. L. & Gruzleski, J. E. The surface tension of molten aluminum and al-si-mg alloy under vacuum and hydrogen atmospheres. *Metall. Mater. Trans. B* **30B**, 1027–1032, <https://doi.org/10.1007/s11663-999-0108-4> (1999).
32. Roach, S. J., Henein, H. & Owens, D. C. A new technique to measure dynamically the surface tension, viscosity and density of molten metals. *Light Met. (Warrendale, PA, U. S.)* 1285–1291 (2001).
33. Gheribi, A. *et al.* Calculating optimal conditions for alloy and process design using thermodynamic and property databases, the factsage software and the mesh adaptive direct search algorithm. *Calphad* **36**, 135–143, <http://www.sciencedirect.com/science/article/pii/S0364591611000563>, <https://doi.org/10.1016/j.calphad.2011.06.003> (2012).
34. Gheribi, A. E., Digabel, S. L., Audet, C. & Chartrand, P. Identifying optimal conditions for magnesium based alloy design using the mesh adaptive direct search algorithm. *Thermochimica Acta* **559**, 107–110, <http://www.sciencedirect.com/science/article/pii/S0040603113000816>, <https://doi.org/10.1016/j.tca.2013.02.004> (2013).
35. Gheribi, A. E. *et al.* Use of a biobjective direct search algorithm in the process design of material science applications. *Optimization and Engineering* **17**, 27–45, <https://doi.org/10.1007/s11081-015-9301-2> (2016).
36. Gheribi, A. E. & Chartrand, P. Thermal conductivity of molten salt mixtures: Theoretical model supported by equilibrium molecular dynamics simulations. *The Journal of Chemical Physics* **144**, <https://doi.org/10.1063/1.4942197> (2016).
37. Gheribi, A. E., Salanne, M. & Chartrand, P. Thermal transport properties of halide solid solutions: Experiments vs equilibrium molecular dynamics. *The Journal of Chemical Physics* **142**, <https://doi.org/10.1063/1.4915524> (2015).
38. Gheribi, A. E., Seifitokaldani, A., Wu, P. & Chartrand, P. An ab initio method for the prediction of the lattice thermal transport properties of oxide systems: Case study of li₂o and k₂o. *Journal of Applied Physics* **118**, <https://doi.org/10.1063/1.4932643> (2015).
39. Seifitokaldani, A. & Gheribi, A. E. Thermodynamically self-consistent method to predict thermophysical properties of ionic oxides. *Computational Materials Science* **108**, Part A, 17–26, <http://www.sciencedirect.com/science/article/pii/S0927025615003626>, <https://doi.org/10.1016/j.commatsci.2015.06.003> (2015).
40. Seifitokaldani, A., Gheribi, A. E., Dollé, M. & Chartrand, P. Thermophysical properties of titanium and vanadium nitrides: Thermodynamically self-consistent approach coupled with density functional theory. *Journal of Alloys and Compounds* **662**, 240–251, <http://www.sciencedirect.com/science/article/pii/S0925838815318107>, <https://doi.org/10.1016/j.jallcom.2015.12.013> (2016).
41. Gheribi, A. Molecular dynamics study of stable and undercooled liquid zirconium based on meam interatomic potential. *Materials Chemistry and Physics* **116**, 489–496, <https://doi.org/10.1016/j.matchemphys.2009.04.020> (2009).
42. Harvey, J.-P., Gheribi, A. E. & Chartrand, P. Accurate determination of the gibbs energy of cu-zr melts using the thermodynamic integration method in monte carlo simulations. *The Journal of Chemical Physics* **135**, 084502, <https://doi.org/10.1063/1.3624530> (2011).
43. Harvey, J.-P., Gheribi, A. E. & Chartrand, P. Thermodynamic integration based on classical atomistic simulations to determine the gibbs energy of condensed phases: Calculation of the aluminum-zirconium system. *Phys. Rev. B* **86**, 224202, <https://doi.org/10.1103/PhysRevB.86.224202> (2012).
44. Levin, E. S., Ayushina, G. D. & Geld, P. V. Density and surface energy polytherms of liquid aluminum. *Teplofiz. Vys. Temp.* **6**, 432–5 (1968).
45. Yatsenko, S. P., Kononenko, V. I. & Sukhman, A. L. Temperature dependence of surface tension and density of tin, indium, aluminum, and gallium. *Teplofiz. Vys. Temp.* **10**, 66–71 (1972).
46. Brillo, J. & Kolland, G. Surface tension of liquid al-au binary alloys. *J. Mater. Sci.* **51**, 4888–4901, <https://doi.org/10.1007/s10853-016-9794-x> (2016).
47. Laty, P., Joud, J. C., Desre, P. & Lang, G. Surface tension of liquid copper-aluminum alloys. *Surf. Sci.* **69**, 508–20 (1977).
48. Somol, V., Franz, F. & Kubicek, L. Surface tension of aluminum-silicon alloys. *Kovove Mater.* **23**, 223–7 (1985).
49. Sarou-Kanian, V., Millot, F. & Rifflet, J. C. Surface tension and density of oxygen-free liquid aluminum at high temperature. *Int. J. Thermophys.* **24**, 277–286 (2003).
50. Rothwell, E. A precise determination of the viscosity of liquid tin, lead, bismuth, and aluminum by an absolute method. *J. Inst. Met.* **90**, 389–94 (1962).

51. Orkvasov, T. A., Ponezhev, M. K., Sozaev, V. A. & Shidov, K. T. An investigation of the temperature dependence of the surface tension of aluminum alloys. *High Temp. (Transl. of Teplofiz. Vys. Temp.)* **34**, 490–492 (1996).
52. Friedrichs, H. A., Ronkow, L. W. & Zhou, Y. Measurement of viscosity, density, and surface tension of metal melts. *Steel Res.* **68**, 209–214, <https://doi.org/10.1002/srin.199701780> (1997).
53. Ibragimov, K. I., Alchagirov, B. B., Taova, T. M., Chocheva, A. M. & Khokonov, K. B. Surface tension of aluminum and its alloys with indium and tin. *Trans. JWRI* **30**, 323–327 (2001).
54. Bian, M., Chen, Q. & Wang, J. Density, surface tension, wettability, and adhesive energy of liquid aluminum and aluminum-rare earth alloys on boron nitride (bn) surface. *Jinshu Xuebao* **24**, B139–B141 (1988).
55. Beranek, M., Sebkova, J. & Somol, V. Surface tension of liquid aluminum-zinc. *Sb. Vys. Sk. Chem.-Technol. Praze, Anorg. Chem. Technol.* **B27**, 153–73 (1982).
56. Assael, M. J. *et al.* Reference data for the density and viscosity of liquid cadmium, cobalt, gallium, indium, mercury, silicon, thallium, and zinc. *J. Phys. Chem. Ref. Data* **41**, 033101/1–033101/16, <https://doi.org/10.1063/1.4729873> (2012).
57. Assael, M. J. *et al.* Reference data for the density and viscosity of liquid antimony, bismuth, lead, nickel and silver. *High Temp. - High Pressures* **41**, 161–184 (2012).
58. Assael, M. J. *et al.* Reference data for the density and viscosity of liquid aluminum and liquid iron. *J. Phys. Chem. Ref. Data* **35**, 285–300, <https://doi.org/10.1063/1.2149380> (2006).
59. Assael, M. J. *et al.* Reference data for the density and viscosity of liquid copper and liquid tin. *J. Phys. Chem. Ref. Data* **39**, 033105/1–033105/8, <https://doi.org/10.1063/1.3467496> (2010).
60. Nasch, P. M. & Steinemann, S. G. Density and thermal expansion of molten manganese, iron, nickel, copper, aluminum and tin by means of the gamma-ray attenuation technique. *Phys. Chem. Liq.* **29**, 43–58, <https://doi.org/10.1080/00319109508030263> (1995).
61. Huang, X., Togawa, S., Chung, S.-I., Terashima, K. & Kimura, S. Surface tension of a si melt: influence of oxygen partial pressure. *J. Cryst. Growth* **156**, 52–8, [https://doi.org/10.1016/0022-0248\(95\)00207-3](https://doi.org/10.1016/0022-0248(95)00207-3) (1995).
62. Keene, B. J., Mills, K. C. & Brooks, R. F. Surface properties of liquid metals and their effects on weldability. *Mater. Sci. Technol.* **1**, 568–71, <https://doi.org/10.1179/026708385790124495> (1985).
63. Lee, H. K., Frohberg, M. G. & Hajra, J. P. Surface tension measurements of liquid iron-nickel-sulfur ternary system using the electromagnetic oscillating droplet technique. *ISIJ Int.* **33**, 833–8, <https://doi.org/10.2355/isijinternational.33.833> (1993).
64. Ownby, P. D. & Liu, J. Surface energy of liquid copper and single-crystal sapphire and the wetting behavior of copper on sapphire. *J. Adhes. Sci. Technol.* **2**, 255–69, <https://doi.org/10.1163/156856188X00264> (1988).
65. Tanaka, T., Nakamoto, M., Oguni, R., Lee, J. & Hara, S. Measurement of the surface tension of liquid ga, bi, sn, in and pb by the constrained drop method. *Z. Metallkd.* **95**, 818–822, <https://doi.org/10.3139/146.018027> (2004).
66. Kasama, A., Iida, T. & Morita, Z. Temperature dependence of the surface tension of pure liquid metals. *Nippon Kinzoku Gakkaishi* **40**, 1030–8 (1976).
67. Eichel, R.-A. & Egry, I. Surface tension and surface segregation of liquid cobalt-iron and cobalt-copper alloys. *Z. Metallkd.* **90**, 371–375 (1999).
68. Matuyama, Y. The surface tension of molten metals and alloys. *Sci. Rep. Tohoku Imp. Univ., Ser. 4* **16**, 555–62 (1927).
69. Abbaschian, G. J. Surface tension liquid gallium. *J. Less-Common Met.* **40**, 329–33, [https://doi.org/10.1016/0022-5088\(75\)90077-6](https://doi.org/10.1016/0022-5088(75)90077-6) (1975).
70. Naidich, Y. V., Perevertailo, V. M. & Obushchak, L. P. Density and surface tension of gold-silicon and gold-germanium alloys. *Poroshk. Metall.* 73–5 (1975).
71. Osiko, T. P. & Alchagirov, B. B. Surface tensions of binary melts of alkali metals. alloys of rubidium with sodium, cesium, and potassium. *Teplofiz. Vys. Temp.* **25**, 609–11 (1987).
72. Bezukladnikova, L. L., Kononenko, V. I. & Torokin, V. V. Density and surface tension of liquid lanthanum, cerium, and praseodymium. *Teplofiz. Vys. Temp.* **27** (1989).
73. Poindexter, F. E. & Kernaghan, M. Surface tension of sodium. *Phys. Rev.* **33**, 837–50, <https://doi.org/10.1103/PhysRev.33.837> (1929).
74. Melford, D. A. & Hoar, T. P. Determination of the surface tensions of molten lead, tin, and indium by an improved capillary method. *J. Inst. Metals* **85**, 197–205, Paper No. 1742 (1957).
75. Wessing, J. J. & Brillo, J. Density, molar volume, and surface tension of liquid al-ti. *Metall. Mater. Trans. A* **48**, 868–882, <https://doi.org/10.1007/s11661-016-3886-8> (2017).
76. Somol, V. & Beranek, M. Surface tension of molten lead-antimony and lead-bismuth alloys. *Sb. Vys. Sk. Chem.-Technol. Praze, Anorg. Chem. Technol.* **B30**, 199–206 (1984).

Acknowledgements

This research was supported by funds from the Natural Sciences and Engineering Research Council of Canada (NSERC) and Rio Tinto Aluminium. Computations were made in the Briaré cluster at the Université de Montréal, managed by Calcul-Québec and Compute Canada.

Author Contributions

A.E.G. wrote the paper. All authors contributed equally in the development of the model. P.C. supervised the project. All the authors discussed the results and reviewed the manuscript.

Additional Information

Competing Interests: The authors declare no competing interests.

Publisher's note: Springer Nature remains neutral with regard to jurisdictional claims in published maps and institutional affiliations.



Open Access This article is licensed under a Creative Commons Attribution 4.0 International License, which permits use, sharing, adaptation, distribution and reproduction in any medium or format, as long as you give appropriate credit to the original author(s) and the source, provide a link to the Creative Commons license, and indicate if changes were made. The images or other third party material in this article are included in the article's Creative Commons license, unless indicated otherwise in a credit line to the material. If material is not included in the article's Creative Commons license and your intended use is not permitted by statutory regulation or exceeds the permitted use, you will need to obtain permission directly from the copyright holder. To view a copy of this license, visit <http://creativecommons.org/licenses/by/4.0/>.

© The Author(s) 2019